Spontaneous formation of density waves in granular matter under swirling excitation

Song-Chuan Zhao (赵松川)[1, a)] and Thorsten Pöschel[2]

[1)] *State Key Laboratory for Strength and Vibration of Mechanical Structures, School of Aerospace Engineering, Xi'an Jiaotong University, Xi'an 710049, China*

[2)] *Institute for Multiscale Simulation, Friedrich-Alexander-Universität, Cauerstraße 3, 91058 Erlangen, Germany*

(Dated: 13 January 2021)

We study here the spontaneous clustering of a submonolayer of grains under horizontal circular shaking. The clustering of grains occurs when increasing the oscillation amplitude beyond a threshold. The dense area travels in a circular fashion at the driving frequency, even exceeds the speed of driving. It turns out that the observed clustering is due to the formation of density wave. The analysis of a phenomenological model shows that the instability of the uniform density profile arises by increasing the oscillation amplitude and captures the non-monotonic dependence of the transition amplitude of the clustering on the global density of the system. Here, the key ingredient is that the velocity of individual grains increases with the local density. The interplay of dissipative particle-particle interaction and the frictional driving of the substrate results into this dependence, which is tested with discrete element method simulations.

Owing to its non-equilibrium nature, granular materials exhibit phenomena of self-organization across orders of magnitude of length scales, from gold panning[1] to astrophysics[2,3]. Those phenomena are largely represented by the clustering instability, non-uniform density distribution developing out of an initially homogeneous state. Clustering has been observed both in freely cooling granular gas[4,5] and in driven systems[6]. Such a collective behavior leads to pattern formation[7], segregation[1,8] and phase separation[3]. Though clustering of granular matter exhibits some generic features across various systems, there are peculiarities in any particular system that need to be taken into account, *e.g.,* the type of energy input[9]. Unraveling the physics mechanism represents a crossroad of hydrodynamics, nonequilibrium statistical mechanics and the phenomenological theory of pattern formation, which has attracted interest over decades. The discovery of new features challenges the existing concepts and theories[10]. One may refer to Ref. 3 and Ref. 11 and references therein for an overview. In this article, we study a submonolayer of beads under horizontal agitations. The constant frictional driving of the substrate distinguishes it from vertically vibrated systems. Strip-like patterns were reported in such systems subjected to a one-dimensional oscillation[7]. Under two-dimensional oscillations, a liquid-solid transition was found, where the solid phase is reached by increasing the oscillation amplitude[8], an example of 'freezing by heating'. However, the mechanism of the spontaneous clustering is still unknown, and the motion within the clustering region is not investigated in details. In this paper, we untangle this issue by combining experiments, a phenomenological model and DEM Simulations.

For the system studied here, there are three experimental parameters: the oscillation strength, the global packing density and the ratio of the grain size to the container size. We first study a reference system specified and later we investigate the influence of various parameters to the system behavior. The

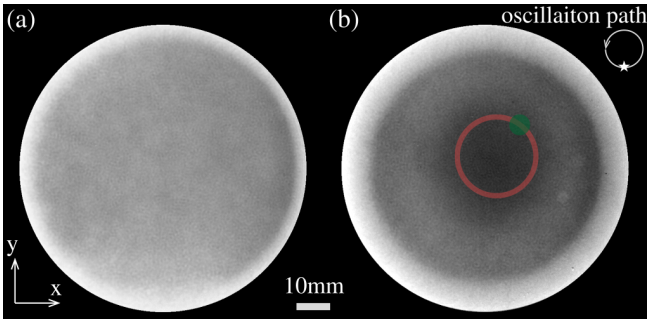

FIG. 1. The average of the experimental images during 10 cycles in the reference frame of the moving container for two oscillation amplitudes: (a) $A = 5$mm and (b) $A = 11$mm. The position of the displayed image in the oscillation cycle is denoted as ★ in the top right inset. Within the cylindrical container the background is bright. The darker a region looks, the denser it is. In (b) the red circle indicates a stationary path of diameter 22πmm *in the lab frame of reference*, along which the local density profile in figure 2a is computed. See the main text for more information. The green solid circle indicates the typical region where individual grains would access during one oscillation cycle. The white circle represents the anti-clockwise oscillation path in scale, whose diameter is 11mm.

submonolayer consists of $N_{tot} = 6930$ polydisperse Zirconium Oxide spheres of diameter $[0.6 \ldots 0.8]$ mm with uniform distribution and the mean $d_g = 0.7$mm. The grains located on an acrylic plate are confined by a 3D-printed PLA circular side wall of diameter $D = 82$mm and height 5mm. The global packing density is given by the area ratio $\phi_{tot} = N_{tot}(d_g/D)^2$. The inclination of the bottom plate is smaller than 0.02 mm/m. The container is subjected to anti-clockwise circular oscillation in the horizontal plane of frequency $f = 5$Hertz. The oscillation amplitude is varied in the range $A = [5 \ldots 13]$mm. Note that here the amplitude represents the diameter of the circular oscillation path (see figure 1b). In this range of agitation and $\phi_{tot} = 0.505$, grains rarely jump over each other and, thus, the packing remains two-dimensional. The system is illuminated by a LED panel from the bottom, and the dynamics

[a)] songchuan.zhao@xjtu.edu.cn

are captured by a high speed camera (Mikrotron MC1362) at the top. The camera is fixed in the laboratory frame of reference. In the following, the analysis is done in this frame for reference.

Upon oscillation grains roll and slide on the substrate and collide with each other and the side wall. The density distribution changes with the oscillation amplitude. Figure 1 shows the average of images of the system during 10 cycles at two oscillation amplitudes. For $A = 5$mm, the system is homogeneous. For $A = 11$mm, a high density region appears at the center. The observed clustering is very sensitive to the oscillation amplitude. It disappears within 10 cycles after decreasing A from 11mm to 10mm. The transition is thus reversible. This highlights the uniqueness of the clustering in the current work with respect to that in a vertically vibrated monolayer[12]. There, hysteresis is observed in the clustering transition. Furthermore, in our experiments the dense area moves anti-clockwise, the same direction as the oscillation (see Supplementary Material).

In figure 1b there are dense areas at the periphery of the packing as well. Those dense boundary layers may be sustained over many cycles and move in a counter-intuitive way, opposite to the swirling motion. This motion mode will be investigated in another work. Nevertheless, the occurrence of a dense area near the periphery is not surprising. The frictional driving of the substrate introduces both linear and angular momentum of grains. The rotational degree of freedom of grains reduces the linear momentum transfer from the substrate[13]. Therefore, grains move slower than the container during oscillation. In consequence, those grains at the periphery of the packing are condensed during certain oscillation phases by the fast moving side wall. In contrast, the spontaneous clustering at the center of the packing can not be explained by this argument. To understand the mechanism of the clustering we study the dynamics of individual particles. To avoid the potential influence of the boundary layers, we exclude particles closer than $15d_g$ to the side wall from the analysis.

To visualize the motion of the dense area, we select a circular path in the lab frame and calculate the local density profile along this path. The path is concentric with the moving line of the center of the bottom plate, but has a larger diameter of 22 mm. The local density ϕ_{loc} is defined for individual grains in a circular neighborhood with a diameter of $5d_g$[14]. The upper bound of ϕ_{loc} is $\phi^* \approx 0.9$ corresponding to the hexagonal packing. ϕ_{loc} along this circular path is plotted versus time in figure 2a. At a given time there is a jump of ϕ_{loc} in space. The maximum of ϕ_{loc} travels along the selected path at the same frequency as the driving (5 Hz). It is noticeable that the length of the selected path is 22π mm, twice the swirling motion of the container $\pi A = 11\pi$mm. In other words, the motion of ϕ_{loc} is faster than the oscillation itself. As explained above, due to the rotational degree of freedom, the grains move slower than the container. This implies that the observed motion is the propagation of density waves. Meanwhile the trajectory of individual grains is still confined to a region much smaller than the size of the oscillation path. For comparison, the region in which a grain on the circular path moves during one cycle is highlighted by the green solid circle in figure 1b. The

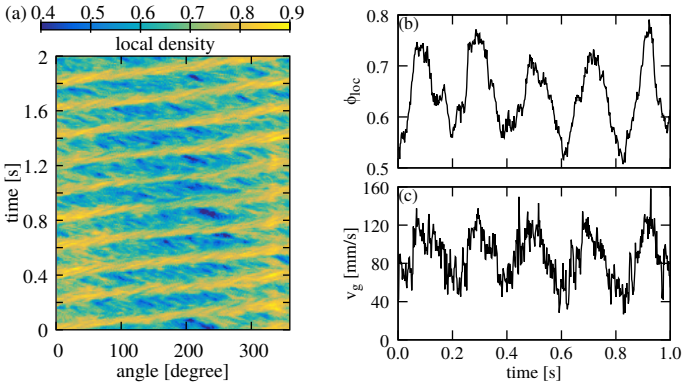

FIG. 2. (a) Local density profile along a circular path versus time for $A = 11$mm and $N_{tot} = 6930$, where clustering at the center is observed. The circular path used here is highlighted in red in figure 1b. The exact position of the path is given in the main text. For the same experiment, the local density ϕ_{loc} and the velocity of a grain v_g on the circular path are plotted versus time in (b) and (c) respectively. See main text for the definition of ϕ_{loc}.

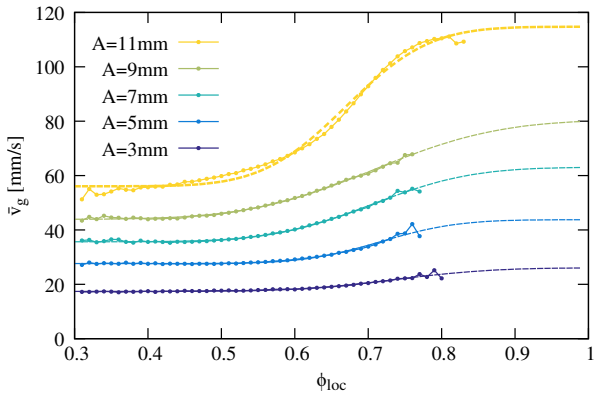

FIG. 3. The presumed value of the velocity of grains, $\bar{v}_g$, increases with the local density, ϕ_{loc}, for various oscillation amplitude A. $A = 11$mm triggers the clustering/density wave at the center of the packing. The dashed lines are fits of the error function to the data.

local density around this grain and its velocity are plotted in figure 2b-c. Its neighborhood experiences periodic compression and dilation. The velocity of the grain, v_g, follows the same periodic pattern and shows a positive correlation with ϕ_{loc}, *i.e.,* grains in denser regions tend to move faster. Figure 3 shows the velocity of the particle as a function of ϕ_{loc} averaged over the region of interest and time (not just of those on the selected circular path). For the experiment in figure 2 ($A = 11$mm) $\bar{v}_g$ saturates for low and high ϕ_{loc}, but increases steeply between $\phi_{loc} = 0.6$ and $\phi_{loc} = 0.8$. Note that a similar dependence of $\bar{v}_g$ on ϕ_{loc} already appears for lower oscillation amplitude ($A < 11$mm), where no clustering/density wave is observed. At low ϕ_{loc}, $\bar{v}_g$ is close to $2/7A\pi f$, as that of a sphere rolling on the oscillating substrate without sliding[13]. Henceforth $\bar{v}_g$ is referred to as the *presumed velocity* of grains.

The dependence of $\bar{v}_g$ on ϕ_{loc} reveals the mechanism lead-

ing to the clustering. Considering the continuity equation:

$$\frac{\partial \phi_{loc}}{\partial t} + \nabla \cdot (\phi_{loc}\vec{v}) = 0. \quad (1)$$

If the velocity of particles tens to relax towards the local presumed velocity $\vec{V}(\phi_{loc})$, it is readily to show that an increasing function of $\vec{V}$ on ϕ_{loc} would promote the formation of shock waves of ϕ_{loc}[15,16]. However, the density wave is only observed for $A \geq 11$mm, which suggests that the collisions between grains introduce an equivalent term of pressure and competes with the promotion of $\vec{V}(\phi_{loc})$. Therefore, the equation for the velocity field can be written as

$$\frac{\partial \vec{v}}{\partial t} + \vec{v}\cdot\nabla\vec{v} = \frac{\vec{V}_g(\phi_{loc}) - \vec{v}}{\tau} - \frac{1}{\phi_{loc}}\nabla p(\phi_{loc}). \quad (2)$$

The first term at the right hand side is the tendency of the local velocity to match the presumed velocity, $\vec{V}_g$, where τ is the time scale of the relaxation of $\vec{v}$ towards $\vec{V}_g$. The implication of this term will be discussed further later. The second term represents the gradient of the pressure, p, arising from the collisions between grains. Note that both $\vec{V}_g$ and p are functions of ϕ_{loc}. The presumed velocity, $\vec{V}_g$, largely follows the direction of the oscillation. It can be seen in figure 2(c) that τ is much smaller than the oscillation period. Therefore, we only consider the flow in the oscillation direction, and Eq. 2 is reduced to a scalar equation.

The model embodied in Eqs. 1 and 2 admits a steady-state solution representing the uniform flow ($\phi_{loc} = \phi_0$ and $v = V_g(\phi_0)$). Such a homogeneous flow is stable against density perturbations, provided[17]

$$(\phi_{loc}V_g')^2 < p'. \quad (3)$$

V_g' and p' are the derivatives of V_g and p with respect to ϕ_{loc}. If condition 3 is violated, the destiny disturbance grows and travels at a higher velocity than $V_g(\phi_0)$ corresponding to homogeneous flow. We use the measured $\bar{v}_g$ a substitute for V_g. Error function is fitted on the data, thus, the derivative, $\bar{v}_g'$ has Gaussian-like peaks. The pressure from collisions is estimated by

$$p = c_0\overline{\delta v_g^2}\frac{d_g^2}{\bar{d}(\bar{d}-d^*)} = c_0\overline{\delta v_g^2}f(\phi_{loc}). \quad (4)$$

with the dimensionless parameter $c_0 \approx 2$ (see Supplementary Material) whose value is later determined by comparing with the experimental observation. For individual grains, the velocity fluctuation δv_g in its neighborhood is extracted. Similar to $\bar{v}_g$, $\overline{\delta v_g^2}(\phi_{loc})$ is the average of δv_g^2 over the region of interest and time for a given ϕ_{loc}. $\bar{d} = d_g/\sqrt{\phi_{loc}}$ represents the average distance between grains for a given ϕ_{loc} and $d^* = d_g/\sqrt{\phi^*}$ corresponds to the hexagonal packing. The fraction on the right hand side of Eq. 4 is purely geometrical and is referred to as $f(\phi_{loc})$ in the following. $f(\phi_{loc})$ increases with ϕ_{loc} and diverges when approaching $\phi_{loc} = \phi^*$. In contrast, though increasing with A, $\overline{\delta v_g^2}$ is largely constant in range of $\phi_{loc} \in [0.3, 0.8]$ for a given A (see Supplementary Material). Therefore, the variant of p is dominated by $f(\phi_{loc})$, and its derivative is approximated by $p' \approx c_0\overline{\delta v_g^2}f'(\phi_{loc})$.

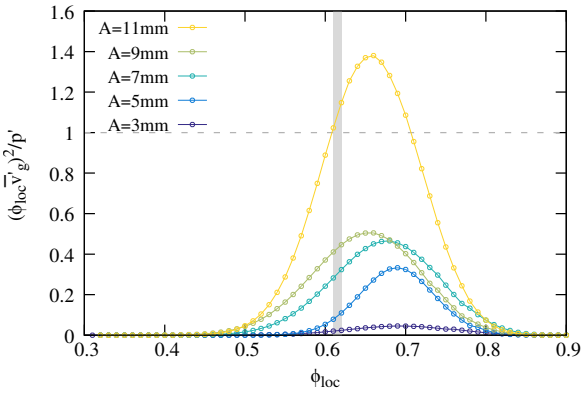

FIG. 4. The ratio of the two terms in Eq. 3 are plotted. The region where the ratio is larger than 1 indicates the violation of Eq. 3. The vertical gray bar indicates the density in the region of interest, ϕ_0, for the oscillation amplitude without clustering.

Figure 4 illustrates the condition Eq. 3. The packing density in the region of interest for $A < 11$mm is indicated by a gray bar ($\phi_0 \in [0.61, 0.62]$). Because particles moves slower than the container/side wall, there is always an empty area not containing grains near the side wall. This empty area can be seen in figure 1a and more salient on the right side of the container in figure 1b. Therefore, ϕ_0 is proportional but larger than ϕ_{tot} in general. $c_0 = 1.8$ is chosen such that Eq. 3 is just violated for $A = 11$mm at ϕ_0, but not for smaller oscillation amplitude. Though both p' (or δv_g^2) and $\bar{v}_g'$ increase with A, the relative increase of the latter is more significant. In consequence, the instability is triggered by increasing A beyond the transition amplitude, A_c. This corresponds to the observed 'freezing by heating'.

Figure 4 provides further insight. The instability associated with the violation of Eq. 3 would only be initialized for packings of intermediate densities, where the ratio $(\phi_{loc}\bar{v}_g')^2/p'$ displays a peak. The peak shape leads to the a non-monotonic dependence of the transition amplitude, A_c, on the global packing density of the system, ϕ_{tot}. Imagine that ϕ_{tot} is increased from 0.505 (analyzed so far) towards ϕ^*. Before reaching the peak of $(\phi_{loc}\bar{v}_g')^2/p'$ the transition amplitude, A_c, would reduce. However, it would raise quickly again when ϕ_{tot} is increased beyond the peak. p' diverges at $\phi_{tot} = \phi^*$, and so does A_c.

The above hypothesis is examined in experiments. The function $A_c(\phi_{tot})$ is plotted in figure 5. The lowest density where spontaneous clustering is observed is $\phi_{tot} \approx 0.505$. The minimum of A_c is reached for $\phi_{tot} \approx 0.64$. The shape of the function $A_c(\phi_{tot})$ is in qualitative agreement with the model. However, the secondary decrease of A_c for $\phi_{tot} \gtrsim 0.7$ is not expected in the model, since the divergence of p at high ϕ_{tot} is supposed to suppress any density wave formation. In practice, when the pressure rising from the collision between grains exceeds that resulting form gravity, grains jump over each other, and the divergence of p and the 2D packing scenario used so

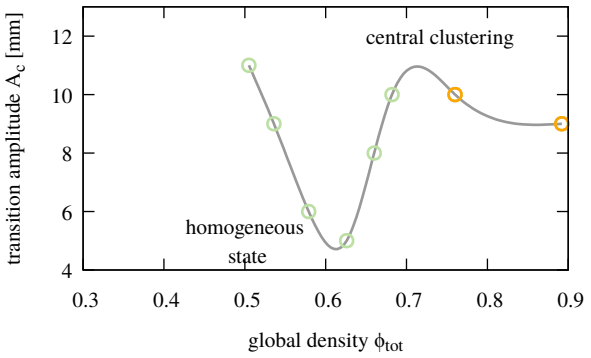

FIG. 5. The transition amplitude, A_c, triggering the clustering is a non-monotonic function of the global packing density ϕ_{tot}. The lowest ϕ_{tot} of the spontaneous clustering is 0.51 for the tested range of A. The last two points where the 2D packing scenario breaks down are highlighted by orange. The solid line serves as guide for the eye.

far breaks down. For dense packings ($\phi_{tot} \gtrsim 0.7$) we observed such behavior near the wall, and the packing density at the center is decreased, which allows the formation of clusters.

We have elaborated the mechanism of clustering by the instability analysis of the uniform flow in a phenomenological model (Eqs. 1 and 2). The key ingredient promoting the clustering is the dependence of the presumed velocity of grains on the the local density. Why does such a dependence exist? We believe that it is a consequence of the interplay between the friction between grains and that between grains and the substrate. μ_{gg} and μ_{gs} denote the friction coefficients of the former and the latter respectively, and F_{gg} and F_{gs} are the corresponding friction forces. Upon agitation F_{gs} accelerates not only the linear momentum but also the angular momentum of individual grains. It has been shown that the rotational degree of freedom effectively reduces the maximum velocity that individual grains could reach by the action of F_{gs} alone[13]. The faster a grain rolls, the slower its linear velocity[7]. Consider now the collision of two grains rolling in the same direction. F_{gg} counteracts the rolling of grains which in turn increases the moment of the inertia with respect to F_{gs} and effectively enhances the linear momentum transfer. F_{gg} is proportional to p, and p increases with ϕ_{loc} and A (Eq. 4). Therefore, grains tend to move faster in dense areas and/or under stronger agitations. These arguments lead to the features of the function $\bar{v}_g(\phi_{loc}, A)$ shown in figure 3, where $\bar{v}_g$ increases with both ϕ_{loc} and A. The velocity of individual particles relaxes towards $\bar{v}_g$ through collisions with others in the cluster, which defines the characteristic time scale τ. In order to further support this line of arguments discrete element method simulations are performed using LIGGGHTS[18]. For a given μ_{gs} and A, the clustering is suppressed by decreasing μ_{gg}. See more information in Supplementary Material.

The clustering phenomenon reported here could be reproduced in experiments with polydisperse grains of diameter 0.8-1 mm, various surface types (smooth and rough glass beads), aspheric grains (e.g., millet seeds) and in a square container. Therefore, the principle of clustering is robust for the explored parameter range. For even larger aspect ratio of d_g/D a solid-like cluster and its reptation motion mode were reported[19,20], which is different from the phenomenology here in both the global density distribution (Fig. 1b) and the motion of the cluster (Fig. 2a). A complete quantitative understanding of the clustering in swirling granular matter, its growth/coarsening and the potential relation to segregation[8] requires further work. In particular, we notice that the presumed velocity includes certain non-local effect, as in the dense phase correlations between velocities of individual particles extend in space. This non-local effect increases with ϕ_{tot} and promotes the significant increase of $\bar{v}_g'$ near A_c. An appropriate hydrodynamic treatment of this term is anticipated in the future research.

This work is supported by German Science Foundation.

The data that support the findings of this study are availablefrom the corresponding authors upon reasonable request.

[1] T. Schnautz, R. Brito, C. A. Kruelle, and I. Rehberg, "A Horizontal Brazil-Nut Effect and Its Reverse," Phys. Rev. Lett. **95**, 028001 (2005).
[2] I. Goldhirsch, "Rapid granular flows," Annu. Rev. Fluid Mech. **35**, 267–293 (2003).
[3] S. Herminghaus and M. G. Mazza, "Phase separation in driven granular gases: exploring the elusive character of nonequilibrium steady states," Soft Matter **13**, 898–910 (2017).
[4] I. Goldhirsch and G. Zanetti, "Clustering instability in dissipative gases," Phys. Rev. Lett. **70**, 1619–1622 (1993).
[5] C. C. Maaß, N. Isert, G. Maret, and C. M. Aegerter, "Experimental investigation of the freely cooling granular gas," Phys. Rev. Lett. **100**, 248001 (2008).
[6] P. B. Umbanhowar, F. Melo, and H. L. Swinney, "Localized excitations in a vertically vibrated granular layer," Nature **382**, 793 (1996).
[7] D. Krengel, S. Strobl, A. Sack, M. Heckel, and T. Pöschel, "Pattern formation in a horizontally shaken granular submonolayer," Granular Matter **15**, 377–387 (2013).
[8] S. Aumaître, T. Schnautz, C. A. Kruelle, and I. Rehberg, "Granular Phase Transition as a Precondition for Segregation," Phys. Rev. Lett. **90** (2003).
[9] R. Cafiero, S. Luding, and H. J. Herrmann, "Two-Dimensional Granular Gas of Inelastic Spheres with Multiplicative Driving," Phys. Rev. Lett. **84**, 6014–6017 (2000).
[10] M. Hummel, *Hydrodynamics of granular gases: Clustering, universality and importance of subsonic convective waves*, Ph.D. thesis, Georg-August-Universität, Göttingen (2016).
[11] I. S. Aranson and L. S. Tsimring, "Patterns and collective behavior in granular media: Theoretical concepts," Rev. Mod. Phys. **78**, 641–692 (2006).
[12] J. S. Olafsen and J. S. Urbach, "Clustering, Order, and Collapse in a Driven Granular Monolayer," Phys. Rev. Lett. **81**, 4369–4372 (1998).
[13] L. Kondic, "Dynamics of spherical particles on a surface: Collision-induced sliding and other effects," Phys. Rev. E **60**, 751–770 (1999).
[14] The conclusion is unchanged for the diameter of the nighbourhood region between $3d_g$ and $7d_g$.
[15] T.-P. Liu, "Nonlinear resonance for quasilinear hyperbolic equation," J Math Phys **28**, 2593–2602 (1987).
[16] S. Friedlander and D. Serre, *Handbook of mathematical fluid dynamics*, Vol. 3 (Elsevier, 2002).
[17] D. A. Kurtze and D. C. Hong, "Traffic jams, granular flow, and soliton selection," Phys. Rev. E **52**, 218 (1995).
[18] C. Kloss, C. Goniva, A. Hager, S. Amberger, and S. Pirker, "Models, algorithms and validation for opensource dem and cfd–dem," Progress in Computational Fluid Dynamics, An Int. J. **12**, 140–152 (2012).
[19] M. A. Scherer, V. Buchholtz, T. Pöschel, and I. Rehberg, "Swirling granular matter: From rotation to reptation," Phys. Rev. E **54**, R4560–R4563 (1996).
[20] M. A. Scherer, K. Kötter, M. Markus, E. Goles, and I. Rehberg, "Swirling granular solidlike clusters," Phys. Rev. E **61**, 4069–4077 (2000).